# Fabrication of Hollow Spheres and Thin Films of Nickel Hydroxide and Nickel Oxide with Hierarchical Structures

**Debao Wang,* Caixia Song, Zhengshui Hu, and Xun Fu**

*College of Chemistry and Molecular Engineering, Qingdao University of Science & Technology, Qingdao 266042, PRC*

*Received: July 20, 2004; In Final Form: October 3, 2004*

Hollow spheres and thin films of $Ni(OH)_2$ and NiO with unusual form and hierarchical structures have been synthesized by a simple solution chemistry method. First, in situ formed $Ni(OH)_2$ nanoflakelets organized on the surface of styrene−acrylic acid copolymer (PSA) latex particles to form core/shell structures. $Ni(OH)_2$ hollow shells built up with nanoflakelets were obtained after subsequent removal of the core latex particles by dissolving PSA latex in toluene; the removal of the cores by calcinations would result in NiO hollow shells, also with hierarchical structures. BET calculation showed the surface area of the NiO hollow spheres was 156 $m^2/g$. The nanoflakelets could also organize themselves into thin films with hierarchical structures. It is anticipated that these novel structures will have some unique applications in Ni-based batteries and other potentials.

## Introduction

Nickel hydroxide ($Ni(OH)_2$), as one of the most important transition metal hydroxides, has received increasing attention due to its extensive applications, especially as a positive electrode active material, in alkaline rechargeable Ni-based batteries.[1] NiO is a very prosperous material, and it has been used in various fields, such as catalysis,[2] battery cathodes,[3] electrochromic films,[4] and fuel cell electrodes.[5] $Ni(OH)_2$ can be conveniently synthesized in solutions of Ni(II), a process which usually involves homogeneous precipitation by employing urea.[6,7] NiO can be conveniently prepared by thermal decomposition of its precursors.[8] As the current research is driving toward nanoscale phenomena and technology, the exploration of new synthesis methods for $Ni(OH)_2$ and NiO nanocrystals with different morphologies will find new applications or improve existing performance. It has been reported that the capacity of the positive electrode could be significantly increased when nanophase $Ni(OH)_2$ was added to micrometer-size spherical $Ni(OH)_2$.[9] Therefore, many reports have concerned the synthesis of $Ni(OH)_2$ and NiO nanocrystals, including nanosized $\alpha$-$Ni(OH)_2$,[10] single-crystalline $Ni(OH)_2$ nanorods and NiO nanorings,[11] $Ni(OH)_2$ and NiO nanosheets,[12a] and nanoribbons.[12b] However, how to synthesize $Ni(OH)_2$ and NiO spheres with hierarchical nanostructures is still a big challenge to chemists.

Recently, morphology-controlled synthesis and the large-scale self-assembly of the nanoscale building blocks into complex structures have been the focus of significant interests in materials chemistry and device fabrications. A number of processes have been reported on the fabrication of common one-, two-, and three-dimensional architectures.[13] Controlled organization of primary building units into curved structures represents another challenge for materials synthesis as a result of their high potential in new technological applications.[14,15]

For the construction of hollow spheres with hierarchical wall structures, surfactants or tri-block copolymers are usually required as structure-directing reagents.[16] Walsh and Mann reported the fabrication of hollow shells of skeletal-structured calcium carbonate from oil−water−surfactant microemulsions using polystyrene beads as the substrate.[17] More recently, Mirkin's group investigated the assembly of rodlike building blocks into curved hollow structures.[18] Liu and Zeng elucidated a two-tiered organizing scheme for the construction of CuO hollow spheres with CuO nanoribbons.[19] Herein, we demonstrate a scheme for the construction of curved architectures with in situ formed $Ni(OH)_2$ nanoflakelets as building blocks. Curved shells built up with building blocks of nanoparticles,[15,20] nanorods,[18] nanoribbons,[19] or skeletal structures[17] have been reported; however, to the best of our knowledge, few reports have concerned the synthesis of $Ni(OH)_2$ and NiO nanoflakelets as nanoscale building blocks for the construction of hollow shells and thin films with hierarchical structures.

## Experimental Section

All the chemicals were of analytical purity and were used as received. Poly(styrene−methyl acrylic acid) (PSA) latex used as core particles was prepared by the radical copolymerization method using ammonium persulfate as the initiator.[21] Figure 2a shows the TEM image of the as-synthesized PSA latex particles with uniform size and diameter of about 600 nm.

Typically, an aqueous solution containing 10.0 g/L of PVP, 0.0024 mol/L of $NiSO_4$, 0.048 mol/L of urea, and 1.8 g/L of PSA latex was aged in capped test tubes at 90 °C for 48 h. After that, the suspension was cooled to room temperature and centrifuged. The precipitates were redispersed into the reaction solution, and the coating procedure was repeated two more times. Finally, the precipitates were washed several times with water and ethanol, respectively, and dried under vacuum at 40 °C to obtain core/shell particles. The coating experiments were conducted under different conditions, and the results are summarized in Table 1. To prepare $Ni(OH)_2$ hollow spheres, the obtained composite particles were dispersed in toluene, then centrifuged and redispersed in toluene. This process was repeated several times to dissolve the PSA cores completely.

* Corresponding author. Tel: +86-532-4022787. E-mail: wangdb@ustc.edu.

10.1021/jp046797o CCC: $30.25 
Published on Web 12/31/2004

**TABLE 1: Summary of Experimental Conditions versus the Products**

| sample no. | $Ni^{2+}$ (mol/L) | alkaline (mol/L) | PVP (g/L) | PSA (g/L) | products |
|---|---|---|---|---|---|
| 1 | 0.0024 | urea, 0.048 | 10.0 | 1.8 | core/shell structures + $Ni(OH)_2$ thin films |
| 2 | 0.0045 | urea, 0.048 | 10.0 | 1.8 | isolated $Ni(OH)_2$ particles + partially coated particles + thin films |
| 3 | 0.0024 | urea, 0.048 | 0.0 | 1.8 | thin films + bare PSA particle |
| 4 | 0.0024 | urea, 0.048 | 10.0 | 0.0 | no reaction |
| 5 | 0.0024 | ammonia, 0.01 | 10.0 | 1.8 | isolated $Ni(OH)_2$ particles + partially coated particles |

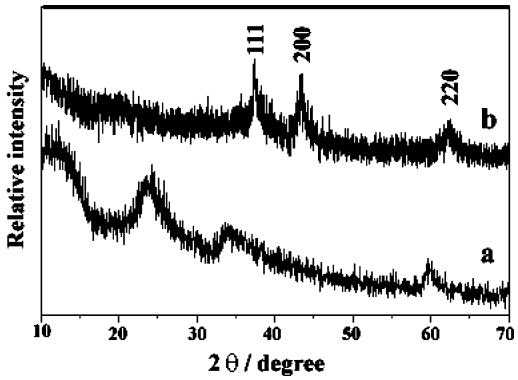


**Figure 1.** XRD patterns of sample 1: (a) before and (b) after calcinations at 600 °C for 2 h.

To obtain NiO hollow spheres, the composite particles were heated to 600 °C at a rate of 1 °C $min^{-1}$ in air and kept at 600 °C for 2 h.

TEM images and electron diffraction (ED) patterns of the samples were taken with a JEM-2000EX (JEOL) transmission electron microscope (160 kV). SEM images were obtained on a JSM-6700F field emission scanning electron microscope equipped with an energy-dispersive X-ray analyzer. X-ray powder diffraction (XRD) patterns were recorded using a Rigaku D/Max r-A X-ray diffractometer with Cu Kα radiation ($\lambda$ = 0.154 178 nm). Thermogravimetric analysis (TGA) was carried out on a TA-50 thermal analyzer (Shimadzu) with a heating rate of 10 °C $min^{-1}$ in flowing air. $N_2$ adsorption was determined by BET measurements using a NOVA-1000e surface area analyzer. Elemental analysis was carried out using a VarioEL III analyzer.

## Results and Discussion

Figure 1, parts a and b, displays the X-ray diffraction (XRD) patterns of an as-synthesized sample (sample 1) before and after calcinations, respectively. No obvious peaks of $\beta$-nickel hydroxide have been observed in Figure 1a, and the main peaks in Figure 1b can be indexed to cubic-phased NiO,[22] suggesting the formation of α-nickel hydroxide[10] and its conversion to cubic-phased NiO.

The morphology of the obtained core/shell particles and the hollow shells was first characterized using a transmission electron microscope (TEM). As can be seen from Figure 2, parts b and c, the core/shell particles in sample 1 have a uniform size and show urchin-like morphology. $Ni(OH)_2$ nanofibers are clearly visible growing on the surface of PSA cores with one cycle of coating reaction (Figure 2b). The individual nanofibers have length of ~40 nm and width of 5−8 nm. To obtain perfect $Ni(OH)_2$ shells, the depositing reaction was carried out for two more cycles. As shown in Figure 2c, $Ni(OH)_2$ nanofibers grow in density, as well as in length (~100 nm) and diameter (~10 nm). More and more fiberlike $Ni(OH)_2$ grow on the surface of the core latex, and a condensed $Ni(OH)_2$ shell is constructed. Because TEM micrographs, even of shadowed samples, do not always reveal the true morphologies of the particles, scanning electron microscope (SEM) images were recorded to reveal the actual structures of the urchin-shaped core/shell particles shown in Figure 2c. As shown in Figure 2d, the core/shell particles are uniform and well-dispersed and have diameters of about 800 nm. Figure 2e shows an SEM image of the core/shell particles in higher magnification. It is clear that the fiberlike coatings under TEM observation are, in fact, constructed with $Ni(OH)_2$ nanoflakelets. The nanoflakelets are found to stand organizing on the surface of PSA particles, thus making them appear as fibers while viewed from TEM images. The thickness and the edge length of the nanoflakelets observed in SEM images are in accordance with the diameter and the length of the nanofibers, respectively, in TEM observations.

$Ni(OH)_2$ hollow spheres were obtained after removing the core latex by dissolving PSA latex in toluene. Figure 3 illustrates a typical TEM image of $Ni(OH)_2$ hollow spheres obtained under this procedure. The urchin-like morphology of $Ni(OH)_2$ shells is sustained very well even after removing the core latex. The obvious contrast between the dark edge and pale center is the evidence for its hollow nature. The wall thickness is about 100 nm. An electron diffraction (ED) pattern in the inset of Figure 3 indicates the polycrystalline nature of nickel hydroxide. Elemental analysis of typical $Ni(OH)_2$ samples gives 2.0% H, 4.4% C, 1.3% N, 0.7% S, and 51.2% Ni, and the formula is found to be $Ni(OH)_{1.26}(CO_3)_{0.31}(OCN)_{0.11}(SO_4)_{0.025}(H_2O)_{0.49}$.

Figure 4 shows the TEM and SEM images of the obtained NiO sample. Hollow particles with obvious contrast between the dark edge and pale center are revealed by the TEM image in Figure 4a. Ringlike ED patterns in the inset of Figure 4a indicate the polycrystalline nature of cubic-phased NiO. The SEM image in Figure 4b indicates that the obtained hollow spheres are relatively uniform and well-dispersed, and the morphology of $Ni(OH)_2$ shells is sustained very well after calcination. The cracked shells in Figure 4b obviously reveal the hollow structure of the calcined particles. Figure 4c represents the SEM image in high magnification to reveal the actual feature of the urchin-like morphology, indicating the presence of NiO nanoflakelets organizing into a honeycomb-like microstructure. BET (Brunauer−Emmett−Teller) surface areas, calculated from nitrogen adsorption isotherms, show that the surface area of the NiO hollow spheres is 156 $m^2/g$, which increases significantly compared with that of the PSA/$Ni(OH)_2$ core/shell particles (23 $m^2/g$) and that of the $Ni(OH)_2$ hollow spheres (62 $m^2/g$). When the core/shell particles were calcined at 900 °C, NiO hollow shells with hierarchical structures could also be sustained perfectly (Figure 4d); however, the total BET surface area decreased to 141 $m^2/g$.

In addition to the core/shell structures, nickel hydroxide thin films with architectural structures have been identified on the wall of the test tubes (Figure 5), which can be easily separated from the core/shell particles by sedimentation of suspension. Figure 5a shows the TEM image of the sheet-type structures, and the thin films seem to be transparent and constructed with $Ni(OH)_2$ nanofibers of ~10 nm in diameter and ~150 nm in length. The SEM image in Figure 5b reveals the actual surface structure of the $Ni(OH)_2$ thin films, which are also constructed

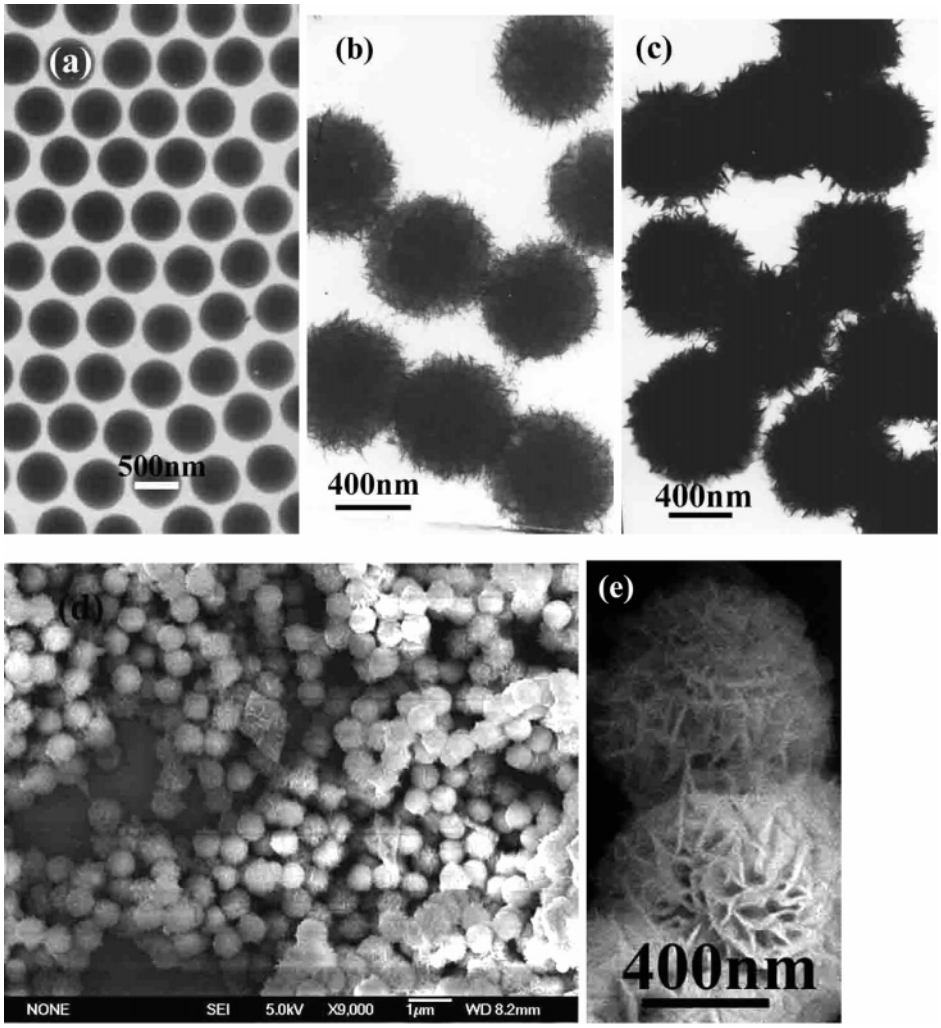


**Figure 2.** (a) TEM image of PSA latex particles, (b) TEM image of sample 1 with one cycle of reaction, and (c) TEM and (d,e) SEM images of sample 1 with three cycles of reaction.

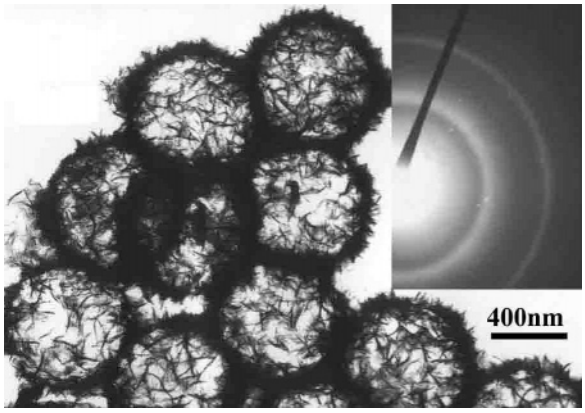


**Figure 3.** TEM image and ED pattern (inset) of the $Ni(OH)_2$ hollow spheres obtained from sample 1.

with $Ni(OH)_2$ nanoflakelets. NiO thin films were obtained by thermal decomposition method at 600 °C for 2 h using the as-synthesized $Ni(OH)_2$ thin films as the precursor. It can be seen from the TEM and SEM images (Figure 5, parts c and d) that the morphology and the characteristics of $Ni(OH)_2$ thin films are sustained perfectly after thermal decomposition to NiO. Although many reports have concerned the deposition of Ni-$(OH)_2$ and NiO thin films,[23] few of them have concerned the deposition of nanoflakelets as building units to assemble into films with architectural morphologies.

It has been reported that negatively charged polystyrene latex can be covered with a smooth inorganic layer by the hydrolysis of metal ions.[24] It is of interest, in our study, that $Ni(OH)_2$ nanoflakelets instead of nanoparticles grow on the surface of the core latex. Although the exact formation mechanism is still unclear, we may just suppose that the formation of $Ni(OH)_2$ nanoflakelets might be related to the nature of its lamellar 2-D structures; as is well-known, $Ni(OH)_2$ is a layered compound of $CdI_2$ type. Urea has been widely used as a Brönsted base[25] for the synthesis of α-nickel hydroxide[6] since the pH value of the medium remains relatively low throughout the process. While aging the reaction solution, urea slightly decomposes[25] and reacts with nickel ions to form $Ni(OH)_2$ nuclei on the surface of PSA templates. The nucleation stage is then followed by diffusion of nickel ions and hydroxide ions to the surface of PSA particles to feed the preferential growth, and $Ni(OH)_2$ nuclei grow into $Ni(OH)_2$ nanoflakelets. At the same time, the nucleation takes place on the wall of the test tube, which leads to the growth of $Ni(OH)_2$ nanoflakelets to construct $Ni(OH)_2$ thin films. In the next cycle of reaction, new nuclei continue generating on the surface of PSA latex and growing into flakelets. As a result, the in situ formed $Ni(OH)_2$ nanoflakelets plant themselves and organize into honeycomb-structured shells or thin films with irregularly shaped pores.

To obtain NiO hollow shells, the removal of core particles and the decomposition of $Ni(OH)_2$ to NiO were performed by calcining the core/shell particles in a stove in air. The thermal

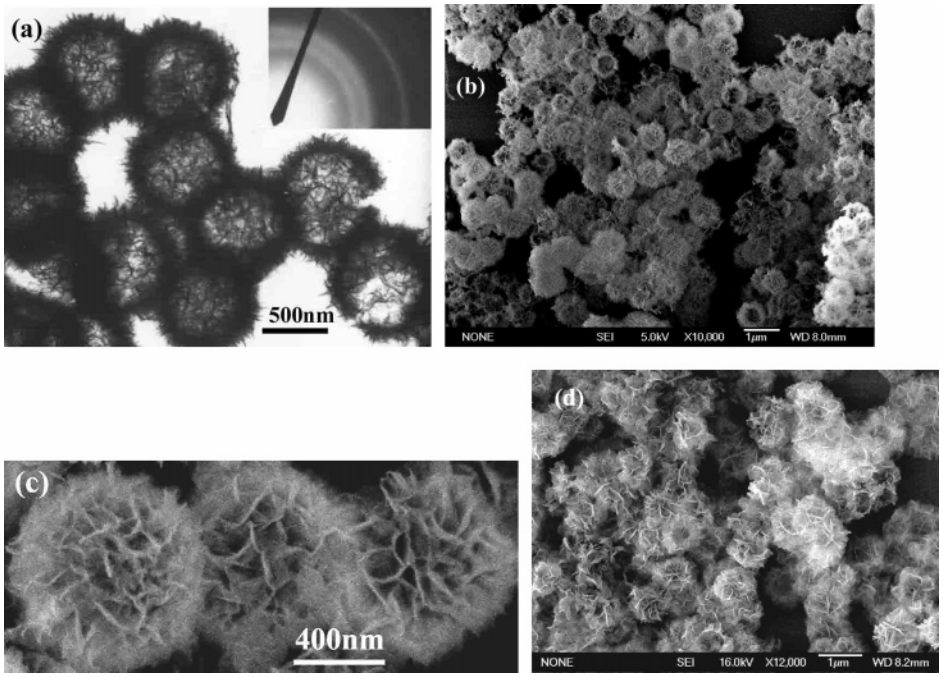


**Figure 4.** (a) TEM image, ED pattern (inset), and (b,c) SEM images of NiO hollow spheres obtained from sample 1 at 600 °C, and (d) SEM images of NiO hollow spheres obtained at 900 °C.

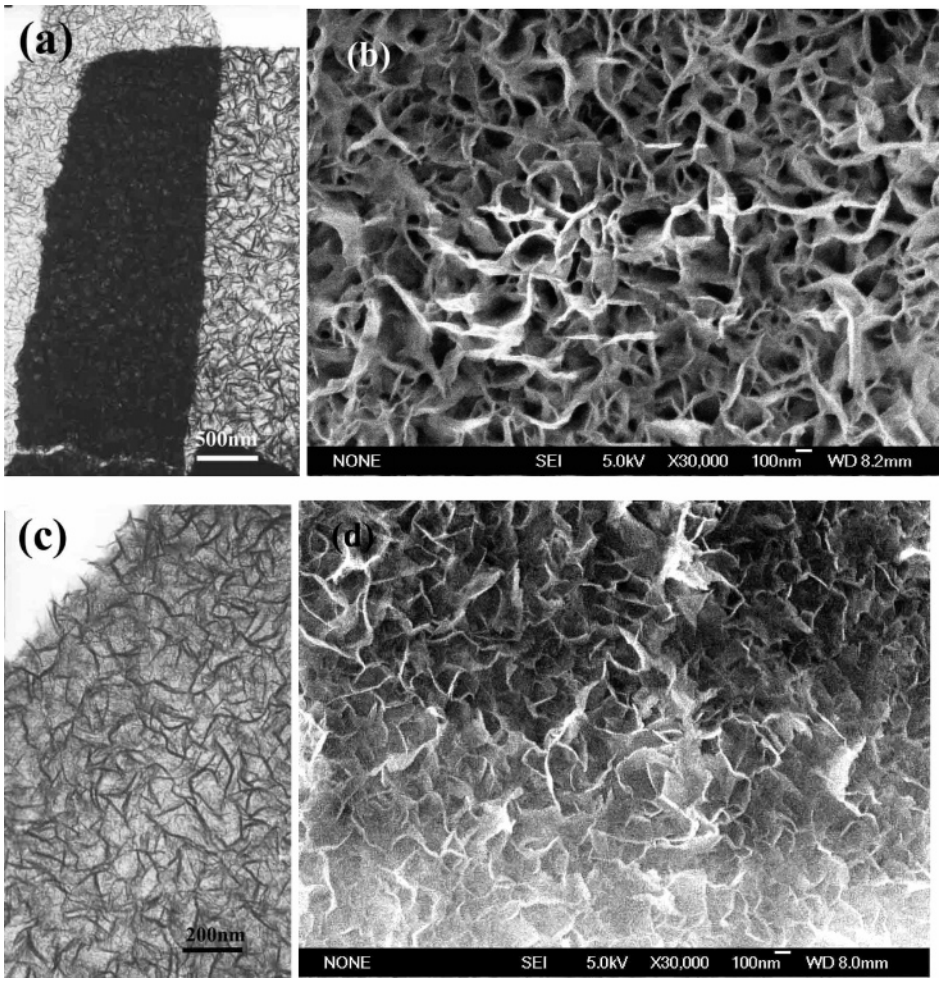


**Figure 5.** TEM and SEM images of (a,b) $Ni(OH)_2$ thin films and (c,d) NiO thin films obtained from sample 1 obtained at 600 °C.

behavior of PSA/$Ni(OH)_2$ core/shell particles (sample 1) was investigated with TGA measurements (Figure 6). It has been reported that the decomposition of $Ni(OH)_2$ to NiO occurs between 298 and 342 °C.[12a] The TGA curve in Figure 6 indicates that there is no obvious weight loss when the temperature is higher than about 600 °C. The calcinations in air result in the

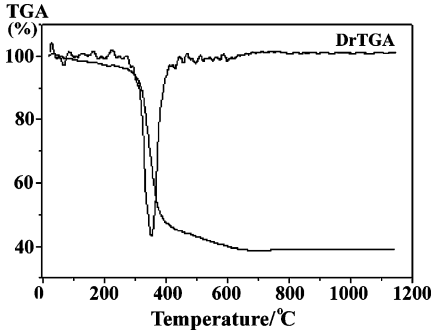


**Figure 6.** TGA curve of sample 1.

decomposition of $Ni(OH)_2$ to NiO and the in situ conversion of $Ni(OH)_2$ nanoflakelets to NiO nanoflakelets, and thus, the morphology and structure of the hollow spheres and thin films sustained very well.

The coating experiments were carried out under different conditions. Table 1 lists the obtained experimental results. We found that urea is irreplaceable for the formation of $Ni(OH)_2$ nanoflakelets as coatings on the core latex. It was believed that hydroxide ions could be released at a suitable rate to feed the growth of $Ni(OH)_2$ nanoflakelets on the core particles. When other alkali conditions (for example, ammonia or NaOH) were used instead of urea, the concentration of hydroxide ions was not easy to control, and $Ni(OH)_2$ was not deposited as coatings on the surface of the core particles, but as isolated $Ni(OH)_2$ particles (sample 5).

Controlled experiments showed that low concentration of nickel ions and more cycles of reaction were necessary to the formation of condensed shells organized with nickel hydroxide nanoflakelets. When the concentration of nickel ions was higher (for example 0.0045 mol/L), isolated nickel hydroxide particles together with the aggregation of partially coated core particles would appear in the products (sample 2). PVP is another factor that has influence on the growth of $Ni(OH)_2$ nanoflakelets as coatings on the surface of the latex particles. For comparison, we performed the experiment with no addition of PVP (sample 3). $Ni(OH)_2$ nanoflakelets were deposited mostly to construct thin films on the wall of the test tubes. We also tried to prepare $Ni(OH)_2$ thin films in the absence of PSA latex particles. However, the reaction did not take place while keeping other conditions constant (sample 4). Further studies are needed to examine the exact roles of PSA particles and PVP molecules for the growth of $Ni(OH)_2$ nanoflakelets as building blocks to assemble into hierarchical structures.

## Conclusion

In summary, the work presented here constitutes a simple method for the fabrication of hollow spheres and thin films of $Ni(OH)_2$ and NiO with unusual form and hierarchical structures. The simplicity is that the aging procedure results in the growth of $Ni(OH)_2$ nanoflakelets as well as their assembly into hierarchical structures. The honeycomb-like structured $Ni(OH)_2$ and NiO would open up the possibility of finding their new applications or improving existing performance, for example, as candidates for studying the nanoarchitecture-dependent performance as cathodes in micro-rechargeable lithium batteries. To this purpose, we are currently investigating the structure of these hollow shells in more detail, as well as the incorporation of functional additives into the shells.

## References and Notes

(1) (a) Ovshinsky, S. R.; Fetcenko, M. A.; Ross, J. *Science* **1993**, *260*, 176. (b) French, H. M.; Henerson, M. J.; Hillman, A. R.; Vieil, E. *J. Electroanal. Chem.* **2001**, *500*, 192.

(2) Sheela, B.; Gomathi, H.; Prabhakara Rao, G. *J. Electroanal. Chem.* **1995**, *394*, 267.

(3) Yoshio, M.; Todorov, Y.; Yamato, K.; Noguchi, H.; Itoh, J.; Okada, M.; Mouri, T. J. *Power Sources* **1998**, *74*, 46.

(4) Miller, E. L.; Rocheleau, R. E. *J. Electrochem. Soc.* **1997**, *144*, 3072.

(5) Makkus, R. C.; Hemmes, K.; Wir, J. H. W. D. *J. Electrochem. Soc.* **1994**, *141*, 3429.

(6) Soler-Illia, G. J. D. A.; Jobbagy, M.; Regazzoni, A. E.; Blesa, M. A. *Chem. Mater.* **1999**, *11*, 3140.

(7) Avena, M. J.; Vazquez, M. V.; Carbonio, R. E.; de Pauli, C. P.; Macagno, V. A. *J. Appl. Electrochem.* **1994**, *24*, 256.

(8) Xiang, L.; Deng, X. Y.; Jin, Y. *Scr. Mater.* **2002**, *47*, 219.

(9) (a) Liu, X. H.; Yu, L. J. *Power Sources* **2004**, *128*, 326. (b) Han, X. J.; Xie, X. M.; Xu, C. Q.; Zhou, D. R.; Ma, Y. L. *Opt. Mater.* **2003**, *23*, 465.

(10) Jeevanandam, P.; Koltypin, Y.; Gedanken, A. *Nano Lett.* **2001**, *1*, 263.

(11) Liang, J. H.; Li, Y. D. *Chem. Lett.* **2003**, *32*, 1126.

(12) (a) Liang, Z. H.; Zhu, Y. J.; Hu, X. L. *J. Phys. Chem. B* **2004**, *108*, 3488. (b) Yang, D. N.; Wang, R. M.; Zhang, J.; Liu, Z. F. *J. Phys. Chem. B* **2004**, *108*, 7531.

(13) (a) Yu, S. H.; Antonietti, M.; Cölfen, H.; Hartmann, J. *Nano Lett.* **2003**, *3*, 379. (b) Gudiksen, M. S.; Lauhon, L. J.; Wang, J.; Smith, D. C.; Lieber, C. M. *Nature* **2002**, *415*, 617. (c) Pileni, M. P. *J. Phys. Chem. B* **2001**, *105*, 3358. (d) Dinsmore, A. D.; Hsu, M. F.; Nikolaides, M. G.; Marquez, M.; Bausch, A. R.; Weitz, D. A. *Science* **2002**, *298*, 1006. (e) Whitesides, G. M.; Grzybowski, B. *Science* **2002**, *295*, 2418. (f) Urbach, A. R.; Love, J. C.; Prentiss, M. G.; Whitesides, G. M. *J. Am. Chem. Soc.* **2003**, *125*, 12704.

(14) (a) Yin, Y.; Rioux, R. M.; Erdonmez, C. K.; Hughes, S.; Somorjai, G. A.; Alivisatos, A. P. *Science* **2004**, *304*, 711.

(15) (a) Caruso, F. *Chem.—Eur. J.* **2000**, *6*, 413. (b) Yin, Y.; Lu, Y.; Gates, B.; Xia, Y. *Chem. Mater.* **2001**, *13*, 1146. (c) Qi, L.; Li, J.; Ma, J. *Adv. Mater.* **2002**, *14*, 300.

(16) (a) Cölfen, H.; Mann, S. *Angew. Chem., Int. Ed.* **2003**, *42*, 2350. (b) Zhu, G.; Qiu, S.; Terasaki, O.; Wei, Y. *J. Am. Chem. Soc.* **2001**, *123*, 7723.

(17) Walsh, D.; Mann, S. *Nature* **1995**, *377*, 320.

(18) Park, S.; Lim, J.-H.; Chung, S.-W.; Mirkin, C. A. *Science* **2004**, *303*, 348.

(19) Liu, B.; Zeng, H. C. *J. Am. Chem. Soc.* **2004**, *126*, 8125.

(20) Nagle, L.; Ryan, D.; Cobbe, S.; Fitzmaurice, D. *Nano Lett.* **2003**, *3*, 51.

(21) Guo, Y.; Gu, G.; Jiao, Y.; Fu, X.; Hu, Z. *Polym. Mater. Sci. Eng.* **2003**, *19* (4), 40 (in Chinese).

(22) JCPDS card no. 78-0643.

(23) Korosec, R. C.; Bukovec, P.; Pihlar, B.; Vuk, A. S.; Orel, B.; Drazic, G. *Solid State Ionics* **2003**, *165*, 191.

(24) Shiho, H.; Kawahashi, N. *Colloid Polym. Sci.* **2000**, *278*, 270.

(25) Shaw, W. H. R.; Bordeaux, J. J. *J. Am. Chem. Soc.* **1955**, *77*, 4729.